Karlsruhe Institute of Technology

Water diffusion in thin silica sheets

- Effect of swelling stress on diffusivity

Theo Fett, Günter Schell

KIT SCIENTIFIC WORKING PAPERS 72

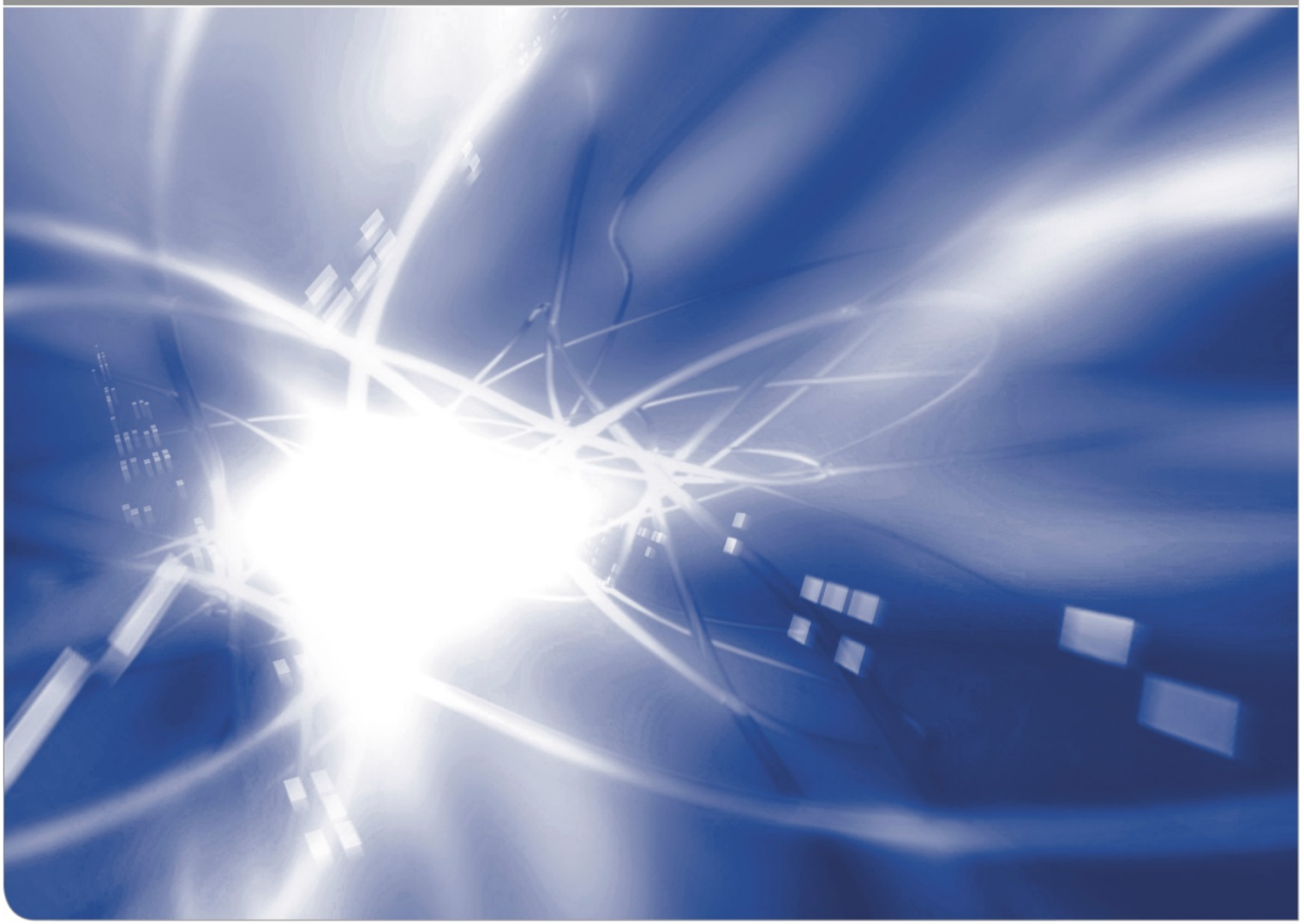

Institut für Angewandte Materialien, IAM
Karlsruher Institut für Technologie (KIT)

Impressum

Karlsruher Institut für Technologie (KIT)
www.kit.edu

2017

ISSN: 2194-1629

Abstract

Water diffuses into silica glass surfaces reacting with the SiO_2 structure under hydroxyl generation. Swelling of water-containing silica at high temperatures was reported in literature. As a consequence of volume swelling and restriction of free expansion by the bulk material, swelling stresses are caused.

The effect of these stresses on diffusivity and equilibrium constant of the water/silica reaction was studied in several papers for thin diffusion layers negligible compared to the thickness of the bulk material.

In very thin glass specimens the diffusion problem becomes more complicated when the diffusion zone size competes with the thickness of the glass specimen. In this case the swelling stresses must decrease with time due to the mechanical equilibrium condition.

In the present investigation we concentrate predominantly on the low-temperature reaction mechanism (<500°C) and apply an analytical solution for transparent first-order considerations. In addition, some first numerical results are reported.

Contents

1. Diffusion and swelling

When H_2O (*l*) comes in contact with silica surfaces, the water diffuses into the glass, and reacts with the silica network [1]

$$\equiv\text{Si-O-Si}\equiv + H_2O \leftrightarrow \equiv\text{SiOH+HOSi}\equiv \tag{1.1}$$

with the concentrations of molecular water, C=[H_2O], and hydroxyl water, S=[SiOH]. For the following considerations, it is assumed that the reaction (1.1) is in equilibrium. The "water" concentration may be represented by the molecular water species.
The equilibrium constant of the reaction (1.1) is at low temperatures, $T \leq 500°C$, represented by the ratio

$$k_1 = \frac{S}{C} \tag{1.2}$$

In the following considerations we assume first that during the diffusion process reaction equilibrium is approached and the *equilibrium constant is not stress-enhanced*.
If the silica/water reaction is in equilibrium, the diffusion of molecular water is governed by the partial differential equation for the uniaxial diffusion

$$\frac{\partial C}{\partial t} = \frac{\partial}{\partial z}\left[D \frac{\partial C}{\partial z} \right] \tag{1.3}$$

where D is the diffusivity and z the depth coordinate. In [2] and [3], we dealt with water diffusion in thick silica specimens with no or moderate stresses. In the present report, we will address thin specimens.
Since the diffusion equation of mass transport has the same form as "heat diffusion" in a solid, the equivalent description as usual for the heat problem can be used. In a previous report we have drawn attention to the fact that surface diffusion of water into silica can be described analytically by introducing mass transfer boundary conditions [3].
According to Carslaw and Jaeger [4] (Section 2.7), the surface condition for temperature reads:

$$\frac{dT}{dz} = -h'(T_0 - T) \quad \text{at } z=0, \tag{1.4}$$

where T_0 is the temperature in the environment, identical with the finally reached temperature for in the body for an infinitely long time, and h' is a normalized heat transfer coefficient, that is for practical use written (see e.g. Chapter 11 in [5]):

$$h' = \frac{h}{\lambda} \tag{1.5}$$

λ is the conductivity for heat transport, the equivalent to the diffusivity D for mass transport. Replacing the temperature by the water concentration C results in

$$\frac{dC}{dz} = -h'(C_0 - C) \quad \text{at } z=0, \tag{1.6}$$

with a parameter h' in (1.4) that is interpreted as a *reaction parameter* for a slow surface reaction that limits the entrance of molecular water species [6] or by a *mass transfer coefficient h* for diffusion [2]:

$$\frac{dC}{dz} = -\frac{h}{D}(C_0 - C) \quad \text{at } z=0, \tag{1.7}$$

Instead of the temperature in the environment, C_0 is here the concentration of molecular water that is asymptotically reached at z=0 for $t\to\infty$. D is an *effective* diffusivity for molecular water that includes the silica/water reaction and h the mass transfer coefficient.

As reported by Shelby [7], hydroxyl generation is accompanied by a reduction of density or equivalently by a volume swelling.

As outlined in [8] the volume swelling strain ε_v is caused by the hydroxyl concentration

$$\varepsilon_v = \tfrac{18}{17}(1+\chi)\frac{S}{2} = \kappa \times S \tag{1.8}$$

with the coefficient $\kappa \cong 0.97$.

A volume element in a plate that undergoes swelling cannot freely expand. If the diffusion zone is small compared to the component dimensions, expansion is completely prevented in the plane of the surface and can only take place normal to the surface plane. This results in an equibiaxial compressive swelling stress, [9]:

$$\sigma_{sw,x} = \sigma_{sw,y} = -\frac{\kappa E}{3(1-\nu)} S = -\frac{\kappa E}{3(1-\nu)} k_1 C \tag{1.9}$$

with a hydrostatic swelling stress σ_h

$$\sigma_h = -\frac{2\,\kappa E}{9(1-\nu)} S = -\frac{2\,\kappa E}{9(1-\nu)} k_1 C \tag{1.10}$$

E is Young's modulus and ν is Poisson's ratio.

The diffusivity is a function of stress, commonly expressed by the hydrostatic stress component, σ_h. The diffusivity for the case of stress-enhanced diffusion is given by the following equation [10]

$$D = D_0 \exp\left[\frac{\sigma_h \Delta V_w}{RT}\right] \tag{1.11}$$

where D_0 denotes the value of the diffusivity in the absence of a stress. T is the absolute temperature in K; ΔV_w is the activation volume for stress-enhanced diffusion and R is the universal gas constant. In the absence of externally applied stresses, the stress in (1.11) is exclusively given by swelling stresses, i.e. $\sigma_h=\sigma_{h,sw}$.
For reasons of simplicity, we introduce a normalized dimensionless time τ, defined by

$$\tau = \frac{h^2}{D_0} t \tag{1.12}$$

2 Diffusion in thin specimens without swelling

In the experimental and theoretical considerations in [2, 3], diffusion in thick specimens was discussed. The diffusion zones were negligible compared to the thickness of the bulk material, $\sqrt{D \times t} << W$, so that the limit-case of a half-infinite body is sufficiently fulfilled.
For *thin specimens* of width $2W$, the zone thickness may be comparable with the specimen thickness. Then the concentration distribution as a function of time reads according to [4]

$$C(z,t) = C_0\left(1 - \sum_{n=1}^{\infty} \frac{2Wh'\cos[\alpha_n(z/W-1)]\sec(\alpha_n)}{Wh'(Wh'+1)+\alpha_n^2} \exp\left[-\alpha_n^2 \frac{D}{W^2} t\right]\right), \quad h' = h/D \tag{2.1}$$

with the time-dependent surface concentration (z=0)

$$C_s(t) = C_0\left(1 - \sum_{n=1}^{\infty} \frac{2Wh'}{Wh'(Wh'+1)+\alpha_n^2} \exp\left[-\alpha_n^2 \frac{D}{W^2} t\right]\right) \tag{2.2}$$

and the average concentration over the cross section

$$\overline{C}(t) = C_0\left(1 - \sum_{n=1}^{\infty} \frac{2(Wh')^2}{\alpha_n^2[Wh'(Wh'+1)+\alpha_n^2]} \exp\left[-\alpha_n^2 \frac{D}{W^2} t\right]\right) \tag{2.3}$$

where C_0 is the saturation value and α_n, n=1, 2, … are the positive roots of

$$\alpha \tan\alpha = Wh' = Wh/D \tag{2.4}$$

In eqs.(2.1-2.4) the parameter Wh/D is equivalent to the Biot number B (sometimes written Bi) for thermal problems:

$$Wh' = \frac{Wh}{D} \equiv B \tag{2.5}$$

Then the equations (2.1-2.4) read

$$C = C_0\left(1 - \sum_{n=1}^{\infty} \frac{2B\cos[\alpha_n(z/W-1)]\sec(\alpha_n)}{B(B+1)+\alpha_n^2} \exp\left[-\alpha_n^2 \frac{\tau}{B^2}\right]\right) \tag{2.1a}$$

$$C_s(t) = C_0\left(1 - \sum_{n=1}^{\infty} \frac{2B}{B(B+1)+\alpha_n^2} \exp\left[-\alpha_n^2 \frac{\tau}{B^2}\right]\right) \tag{2.2a}$$

$$\overline{C}(t) = C_0\left(1 - \sum_{n=1}^{\infty} \frac{2B^2}{\alpha_n^2[B(B+1)+\alpha_n^2]} \exp\left[-\alpha_n^2 \frac{\tau}{B^2}\right]\right) \tag{2.3a}$$

where now α_n, $n = 1, 2, \ldots$ are the positive roots of

$$\alpha \tan \alpha = B \tag{2.4a}$$

The water concentration profiles as a function of time are shown for B=1 in Fig. 1a and B=10 in Fig. 1b in normalized representation. After a normalized time of τ=0.03, the diffusion fronts from the opposite surfaces start to interfere noticeably. With increasing Biot number the concentration differences between surface and centre increase.

The water concentration at the surface, C_s, is given in Fig. 1c for several Biot numbers. At first sight, these results may appear somewhat astonishing since for increasing Biot numbers the surface concentrations at a fixed time τ decrease. For constant D and W, this says that C_0 decreases with increasing mass transfer coefficient h. In this context, it has to be noticed that the normalized time τ also includes the parameter h via $\tau \propto h^2$, so that for short normalized times, the curves become independent of h. This is visible from Fig. 1c. Figure 1d shows results of C_s for small values of B with the abscissa τ/B^2 instead of τ. These curves now show the properties to be expected intuitively.

Since the water uptake m_C is proportional to the average water concentration over the cross-section, it holds simply

$$\frac{m_C}{m_0} = \frac{\overline{C}}{C_0} \tag{2.6}$$

with the average water concentration $\overline{C}$:

$$\overline{C}(t) = \tfrac{1}{2W} \int_0^{2W} C(z,t)\,dz \tag{2.7}$$

and the saturation uptake m_0.

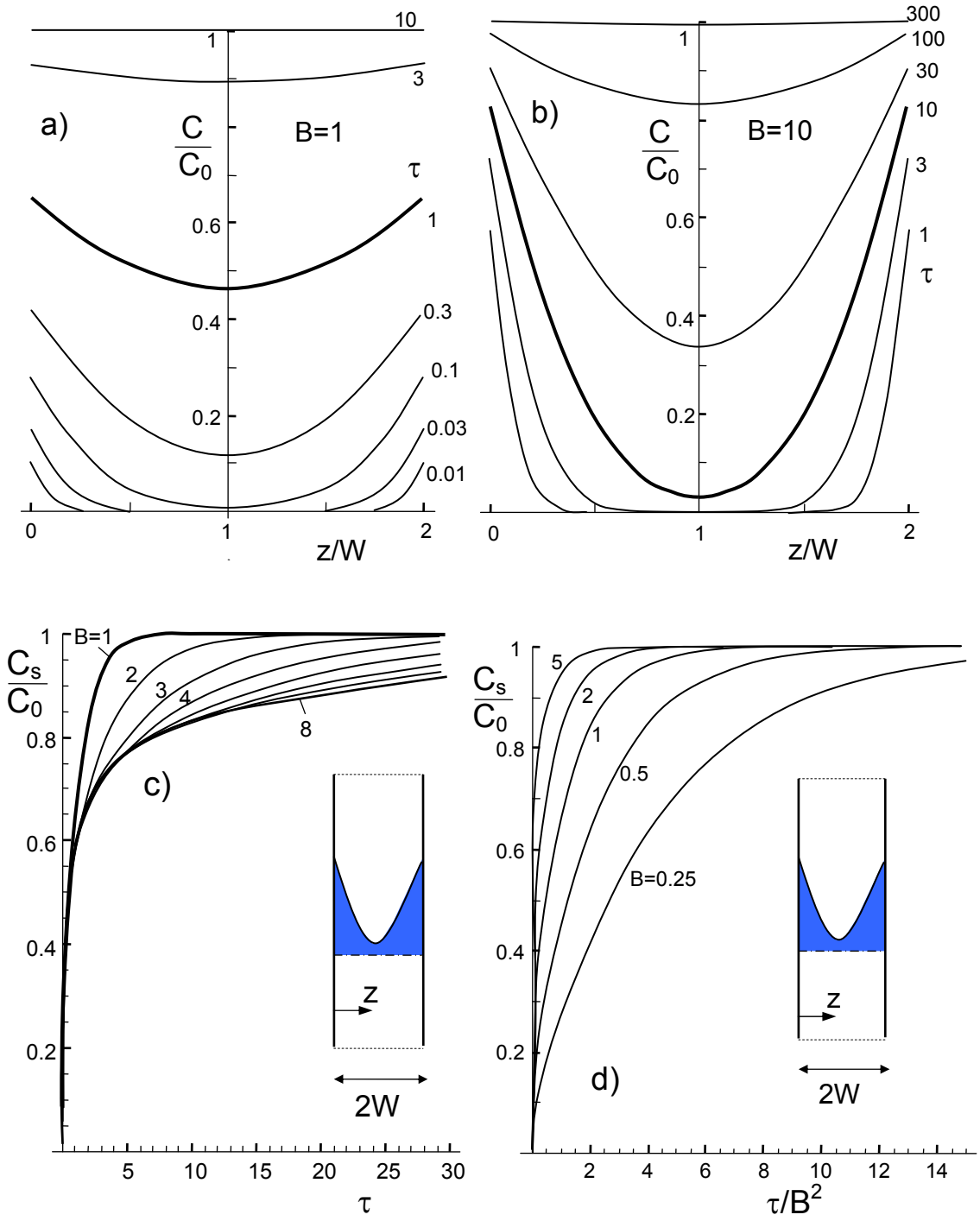

Fig. 1 a), b) Concentration profiles for $D \times t/W^2 = \tau/B^2 = 1$ and 10 for different normalized times τ, c) normalized surface concentrations C_s/C_0 vs normalized time for different Biot numbers, d) results with modified abscissa scaling τ/B^2 for small Biot numbers.

The molecular water uptake as a function of normalized time τ and Biot number is given in Fig. 2a and Fig. 2b for τ and τ/B chosen as the abscissa. As a characteristic feature of the effect of a limited water transfer coefficient *h,* the curves do not start linearly. The surface concentrations increase for short times $\propto\sqrt{t}$ and the layer thickness goes with $\sqrt{t}$, too. This makes that the uptake is proportional to time. In a plot

with $\sqrt{t}$ as the abscissa, the curve shape goes with a quadratic dependency. This effect is also visible from literature results by Davis and Tomozawa [11] that are re-plotted in Fig. 2c

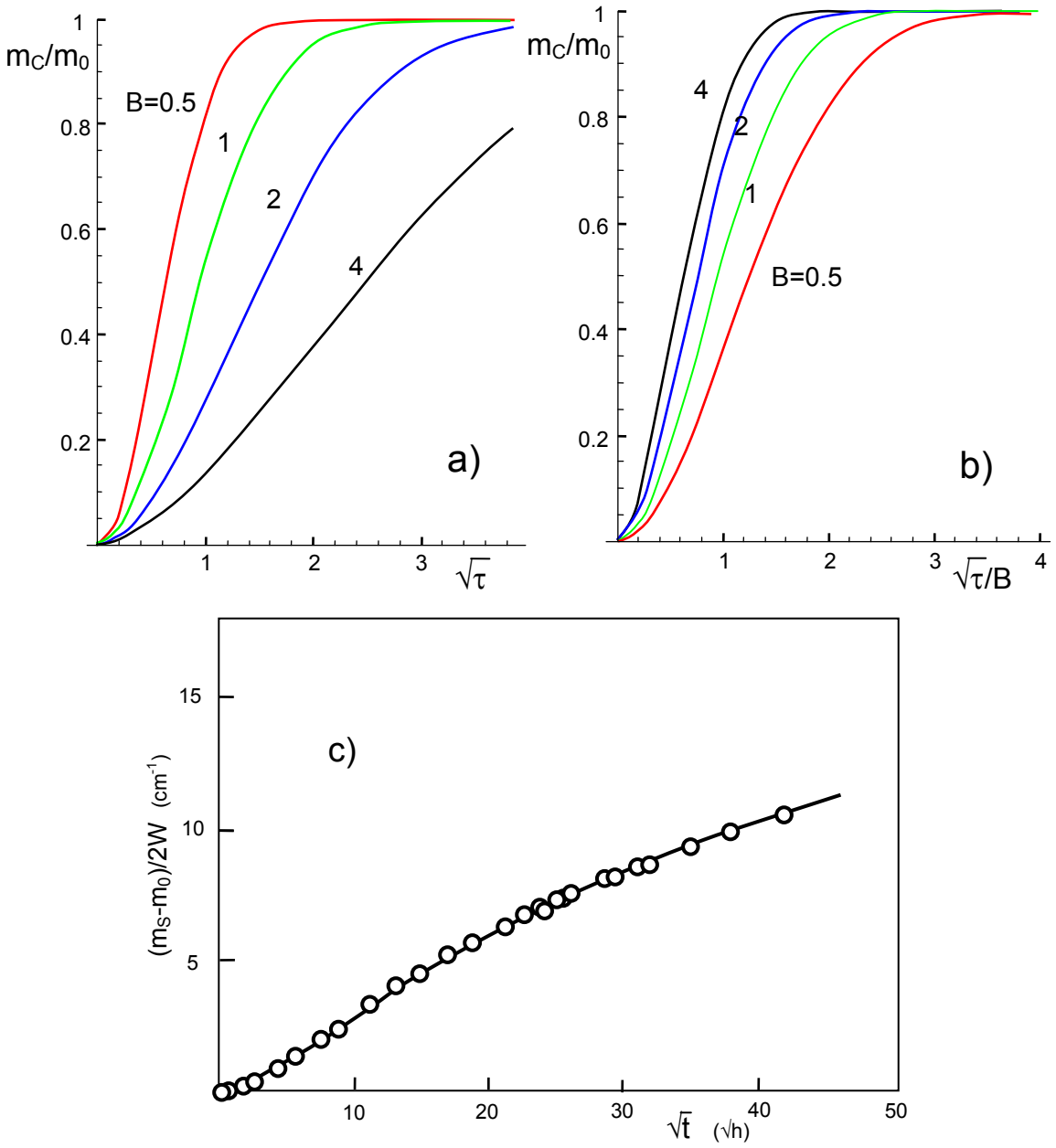

Fig. 2 a) Water uptake m_C/m_0 as a function of normalized time τ and Biot number B, b) the same results with different abscissa, c) measurements by Davis and Tomozawa [11].

3. Swelling stresses in thin specimens

The swelling stresses given by eq.(1.9, 1.10) are valid for the case of thin swelling layers negligible compared with the specimen widths. Now let us consider thin specimens. In this case, the negative hydrostatic swelling stresses in the surface region where the diffusion zones develop must decrease after longer time. This is due to the

fact, that all stresses must disappear when a constant water concentration is reached after long times. Then no restrictions on swelling are possible and the specimen can freely expand. The diffusivity trivially must tend to the value D_0 valid for $\sigma_h=0$.
The condition of mechanical equilibrium requires for the total stress distribution over the thickness that

$$\int_0^{2W} \sigma \, dz = 0 \tag{3.1}$$

This condition is fulfilled by the effective swelling stress σ_{eff}

$$\sigma_{eff}(z) = \sigma_{sw}(z) - \overline{\sigma}_{sw} = -\frac{1}{3}\frac{E}{1-\nu}(\varepsilon_v - \overline{\varepsilon}_v) \tag{3.2}$$

as can simply be validated by inserting (3.2) into (3.1).
In case of the low-temperature reaction with equilibrium constant k_1 it holds for equi-biaxial swelling stress

$$\sigma_{sw,0} = -\frac{1}{3}\frac{E\kappa k_1 C_0}{1-\nu} \tag{3.3}$$

As a consequence of eqs.(3.2) and (3.3), it can be written

$$\frac{\sigma_{eff}(z,t)}{\sigma_{sw,0}} = \frac{C(z,t) - \overline{C}(t)}{C_0} \tag{3.4}$$

For stress-enhanced swelling the equilibrium constant k_1 depends on the swelling stress, $\sigma_{sw} \propto S$. Therefore, it must hold

$$\frac{\sigma_{eff}(z,t)}{\sigma_{sw,0}} = \frac{S(z,t) - \overline{S}(t)}{k_{1,0} C_0} \tag{3.4a}$$

where $k_{1,0}$ is the equilibrium constant in the absence of any stress.
Figure 3 shows the influence of the time on the stress distributions (Figs. 3a, 3b) and the stresses at the surface (Fig. 3c). The stress values are scaled with the swelling stress $\sigma_{sw,0}$ that would occur at the surface of a semi-infinite body for $t \to \infty$.
Figure 3a represents the deviations of the local water concentrations of Fig. 1a from the average value for a Biot number of B=1, i.e. the right hand side of eq.(3.4). The black curves show the results for times before the maximum surface value and the red ones illustrate the distributions after the maximum. Figure 3c gives the surface values as a function of normalized time τ for different B.

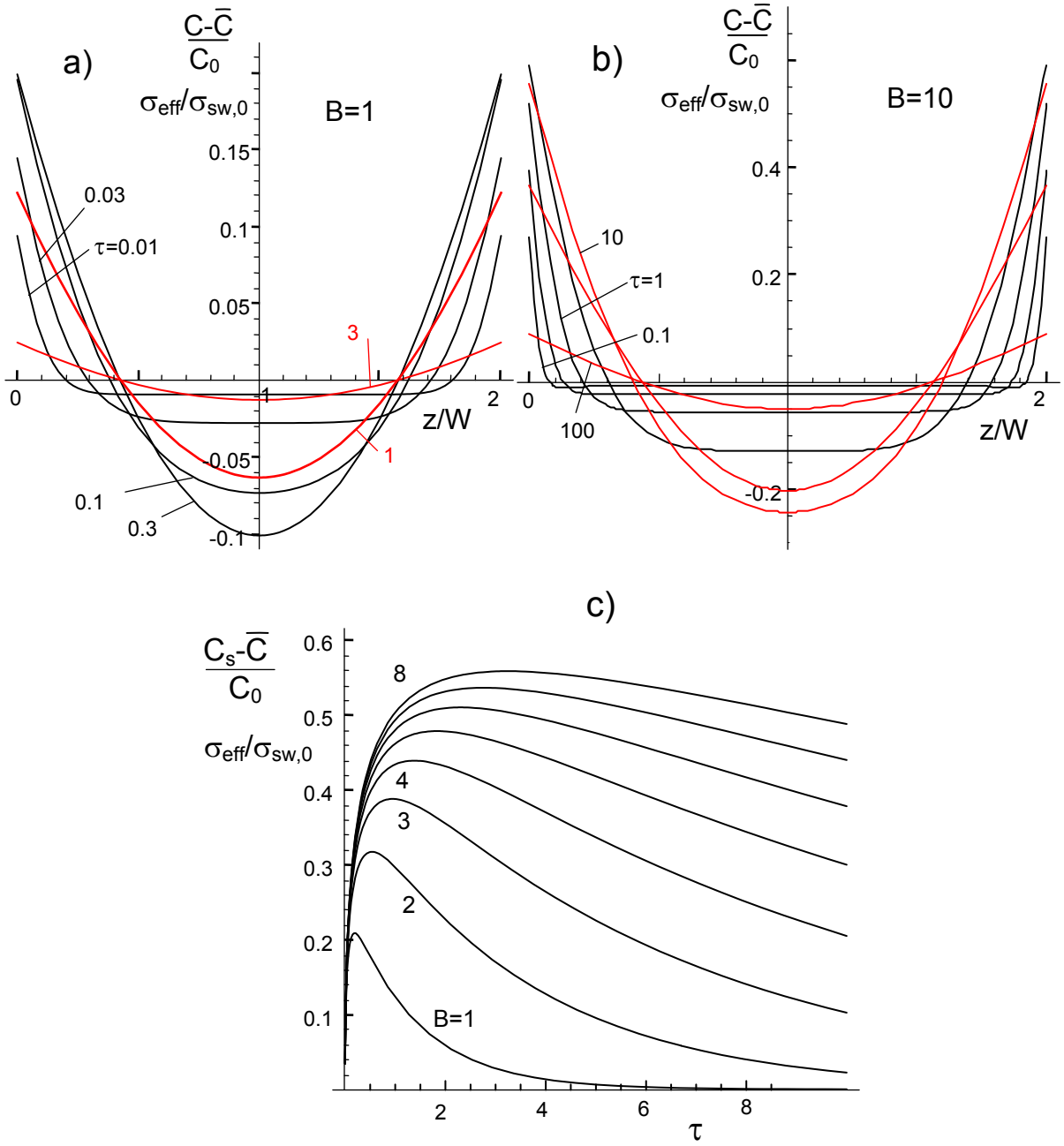

Fig. 3 a) Deviations of concentrations from their average over the width. Black curves: before maximum is reached, red curves: after the maximum (the ordinates are proportional to the swelling stresses), b) concentrations for *B*=10 dependency of surface values with time, c) difference between surface and average concentration.

4. Expectations from limit case considerations

Swelling of silica has several consequences on material behaviour. Two effects on diffusion behaviour may be addressed in this section. Since the analytical solution by the eqs.(2.1a) to (2.4a) does not include stress effects, these equations allow only to perform first-order estimations.

In [12] we could show that the surface water concentration increases at the surface under compressive stresses and decreases under tensile stresses. These findings are a simple consequence of the *limited mass-transfer* coefficient [2] or *slow-reaction* boundary condition [6] at the silica surface.

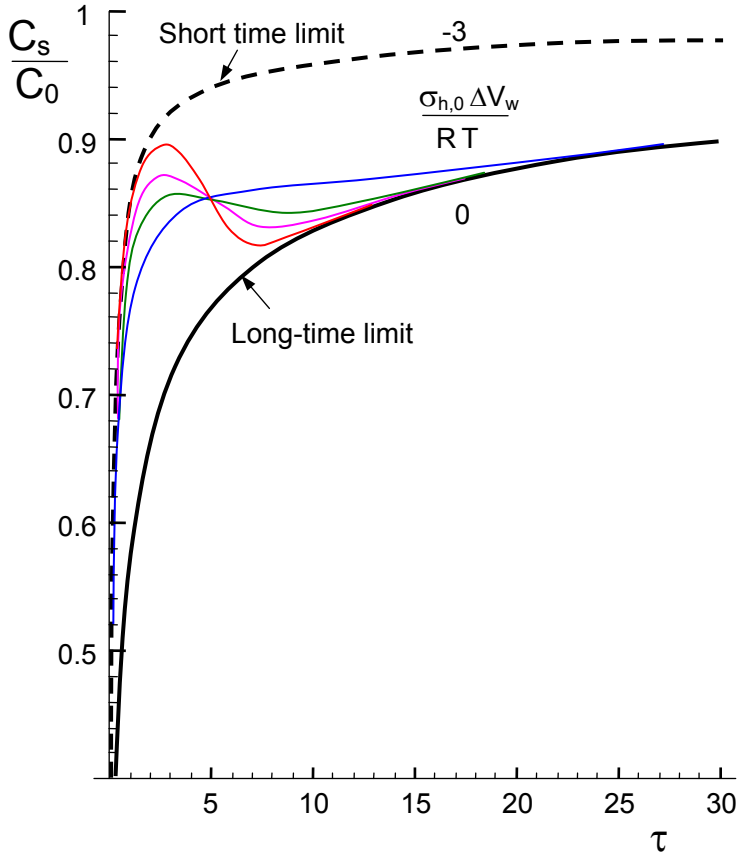

Fig. 4 Effect of diffusion boundary conditions at the silica surface and stress-affected diffusivity, eq.(1.11), on the normalized surface concentration of water, $C_s(\tau)/C_0$. Dashed curve: Limit case for the half-space under swelling at the surface; Solid curve: Limit case for diffusion in the absence of swelling stresses; Coloured curves: Possible limit-case interpolations.

Two limit cases may be considered:

(1) For very short times, t, the thickness of the water diffusion zone, $b=(D\times t)^{1/2}$ is small compared to the specimen thickness, $b<<W$. Consequently, diffusion behaves like in a semi-infinite body. This limit case was outlined in [12]. The surface concentration C_s for $\sigma_{h,0}\Delta V_w/RT=-3$ in eq.(1.11) is shown in Fig. 4 as the dashed curve.

(2) For very long times, the specimen is completely soaked by water, resulting in the concentration $C(z,t)\rightarrow C_0$. Any swelling stress must disappear in the specimen as a consequence of mechanical equilibrium, eqs.(3.2, 3.4). The solution for the half-

space, computed with a disappearing stress-enhancement of $\sigma_{h,0}\Delta V_w / R\,T = 0$, is represented in Fig. 4 by the solid limit curve.

The real diffusion behaviour must start on the dashed curve for short times and tend to the solid curve for long times. This is schematically indicated by the coloured thin curves. Depending on the material parameters this change can occur very slowly (blue curve) or more abruptly (red curve).
From Fig. 4 it can be expected that for long times for which the layer thickness b and the specimen width W become comparable, a maximum in the surface concentration $C(t)$ occurs.

5. Numerical results for stress-enhanced diffusivity

5.1 Results for low temperatures $T \leq 500°C$

Equation (1.3) was numerically solved using the *Mathematica* procedure *NDSolve* [13]. Two boundary conditions had to be satisfied simultaneously, namely

$$\frac{dC}{dz} = -\frac{h}{D}(C_0 - C) \quad \text{at } z=0, \tag{5.1}$$

$$\frac{dC}{dz} = +\frac{h}{D}(C_0 - C) \quad \text{at } z=2W, \tag{5.2}$$

In the following considerations, it is assumed that the coefficient h might be independent of stress. The swelling stress related to a certain concentration C is

$$\sigma_{h,sw} = \sigma_{h,0}\frac{C}{C_0} \quad , \quad \sigma_{h,0} = \sigma_{h,sw}(C_0) \tag{5.3}$$

where the quantity $\sigma_{h,0}$ is the hydrostatic swelling stress value reached for $C=C_0$.

Figure 5 shows the surface values of the effective swelling stresses defined by eq.(3.4) as a function of time τ, Biot number B and hydrostatic swelling stress $\sigma_{h,0}\Delta V_w/RT=-3$. The upper limit curve with $B\to\infty$ represents the case of the half-space, since $B \propto W$. In this case, any diffusion layer is small compared to the specimen width and an unloading effect with increasing layer thickness is impossible.
Figure 6 gives the surface concentration as a function of time τ and Biot number B. An interesting effect is visible for stronger swelling as illustrated in Figs. 6a-6c for several Biot numbers. These figures show a relative concentration maximum, followed by a temporary decrease of $C(0)$. For large times the concentration C_0 is asymptotically approached.
So far, it is not possible to compare the computations of Fig. 6 with experimental results. To our knowledge, the measurements by Davis and Tomozawa [11] in Fig. 2c

are the only data on thin specimens in the temperature region θ<500°C. Due to the rather small diffusivity at 350°C, much longer times are necessary to reach saturation of water uptake.

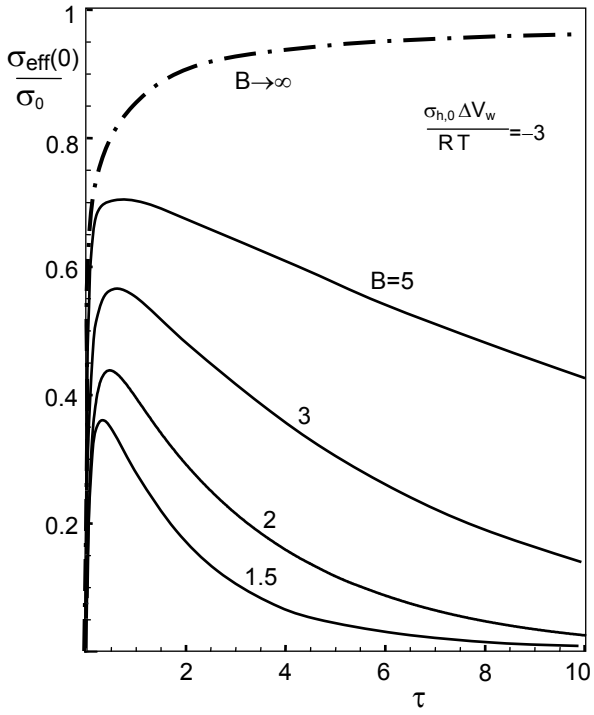

Fig. 5 Effective swelling stresses at the surface.

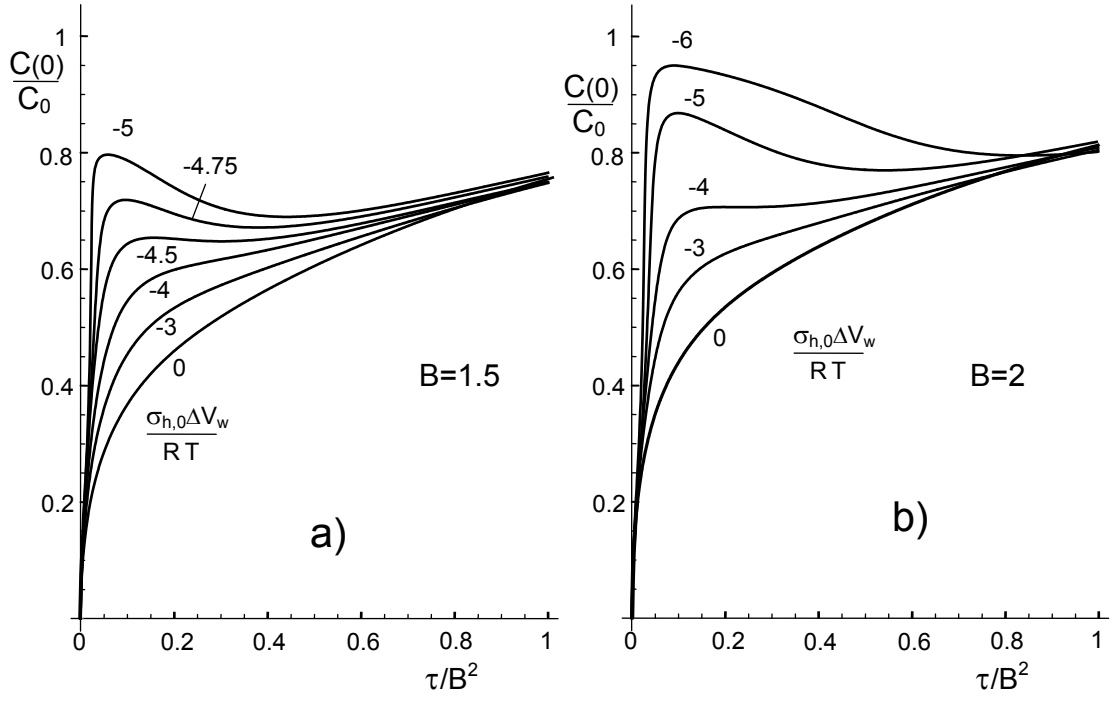

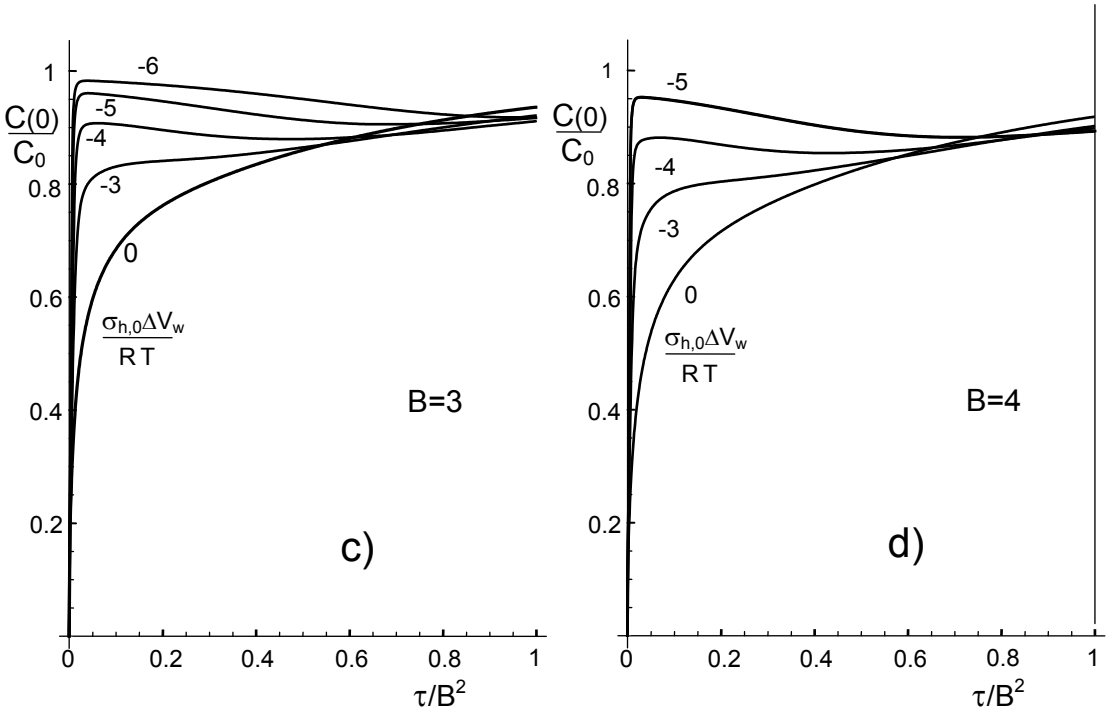

Fig. 6 Water concentration at the surface (effect of swelling stress, Biot number B, and time τ).

The experimental database is better in the temperature region θ>500°C. This is especially the case for θ≥650°C due to the investigations by Davis and Tomozawa [11]. We plan to repeat our computations in the high-temperature region where the analysis is expected to be more complicated due to the fact that $S \propto C^{1/2}$.

5.2 First results for temperatures *T*>500°C

The equilibrium constant of the reaction (1.1) is at high temperatures, T>500°C, represented by the ratio

$$k_2 = \frac{S^2}{C} \tag{5.4}$$

Also in this case we assume that the *equilibrium constant is <u>not</u> stress-enhanced*.
Results of S as a function of swelling stresses are given in Figs. 7a and 7b. The influence of Biot number is shown in Fig. 7c. In principle the same behaviour is visible as in the case of lower temperatures. In Figure 7 the asymptotically reached maximum hydroxyl content is denoted as S_0 given by

$$S_0 = \sqrt{k_2 C_0} \tag{5.5}$$

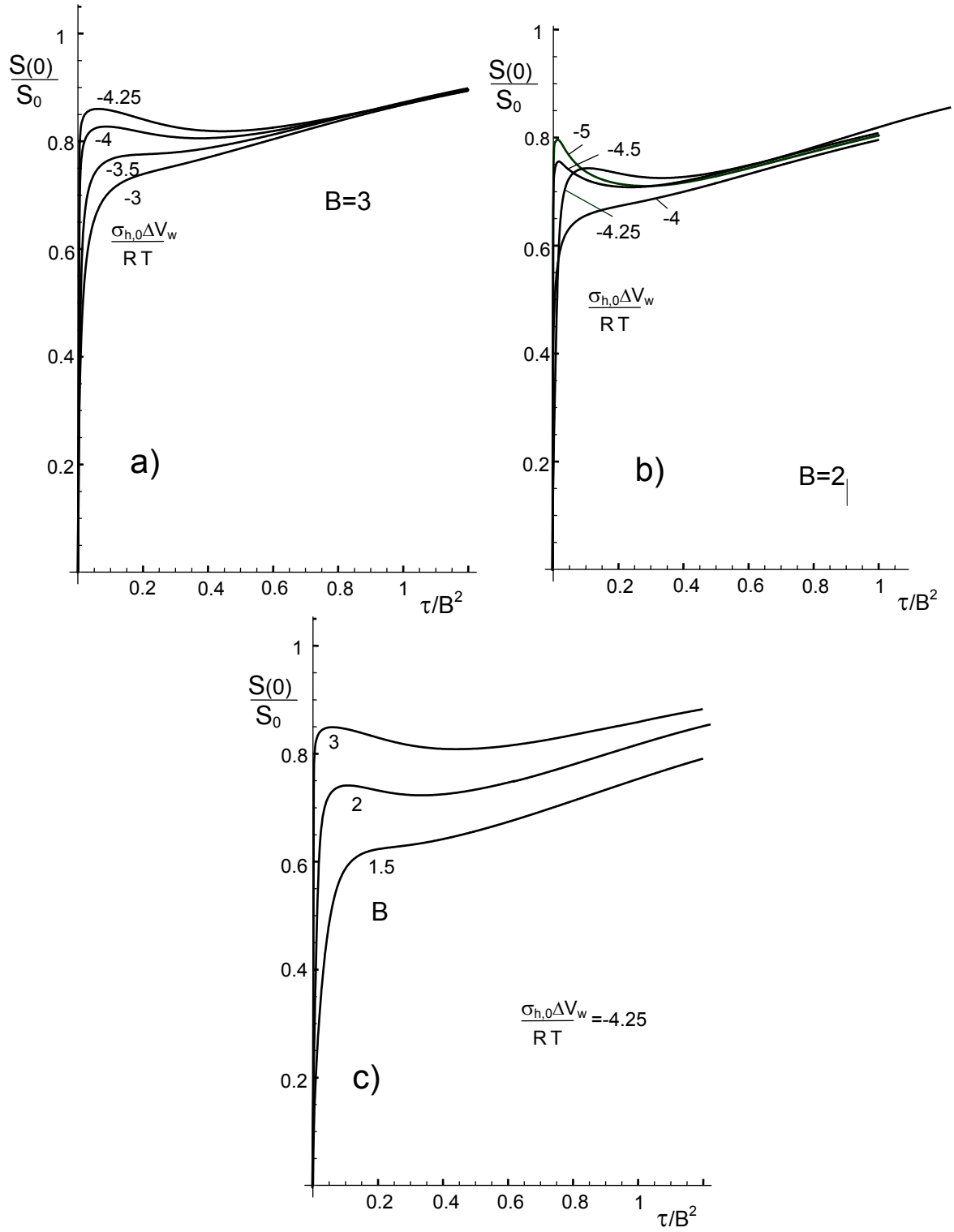

Fig. 7 Hydroxyl concentration at the surface, a) b) effect of swelling stress, c) effect of Biot number.

APPENDIX

Effect of stress-enhanced equilibrium constant

Beside stress-enhanced diffusivity, also the equilibrium constant of eq.(1.1), defined via eq.(1.2), must be stress-dependent, as can be concluded from the principle by Le Chatelier [14]. For volume expansion by swelling, this principle says that under tensile stresses the equilibrium constant k_1 is increased and under compressive stresses decreased.

An approximate analytical solution can be obtained following the general procedure usual in perturbation theory. If we consider the equilibrium constant k_1 as the disturbance parameter, perturbation theory suggests to solve the problem in the absence of stresses, i.e. for $k_1=k_{1,0}$ =const. and to insert the stress-dependent disturbance parameter into this solution. The analytical solution of the undisturbed problem in terms of molecular water is $C(z,t)$ given by eq.(2.1a-2.4a).

The uptake of molecular water, m_C, is obtained from eq.(2.3a)

$$m_C = \overline{C}(t) \times 2W = m_{C,0}\left(1 - \sum_{n=1}^{\infty} \frac{2B^2}{\alpha_n^2[B(B+1)+\alpha_n^2]} \exp\left[-\alpha_n^2 \frac{\tau}{B^2}\right]\right) \tag{A1}$$

where the asymptotically reached value of molecular water uptake is

$$m_{C,0} = 2WC_0 \tag{A2}$$

In the ***absence of stresses*** the hydroxyl water concentration simply results from eq.(1.2)

$$S(z,t) = k_{1,0} C(z,t) \tag{A3}$$

and the related hydroxyl water uptake reads:

$$m_S(t) = k_{1,0} m_C(t) \tag{A4}$$

In ***presence of stresses*** the equilibrium constant is

$$k_1 = k_{1,0} \exp\left[\frac{\sigma_h \Delta\overline{V}}{RT}\right] \tag{A5}$$

with the hydrostatic stress in first order

$$\sigma_h = -\frac{2\kappa E}{9(1-\nu)} k_{1,0} C \tag{A6}$$

according to eq.(1.10) and the partial molar volume $\Delta\overline{V}$ for the hydroxyl.

The solution for the hydroxyl water uptake under swelling stresses is then given by

$$m_S(t) = k_{1,0} \int_0^{2W} C(z,t) \exp\left[\lambda C_0 \left(\frac{C(z,t) - \overline{C}}{C_0}\right)\right] dz \tag{A7}$$

with the abbreviation λ

$$\lambda = -\frac{2}{9} \frac{\kappa E \Delta \overline{V}}{(1-\nu) RT} k_{1,0} \tag{A8}$$

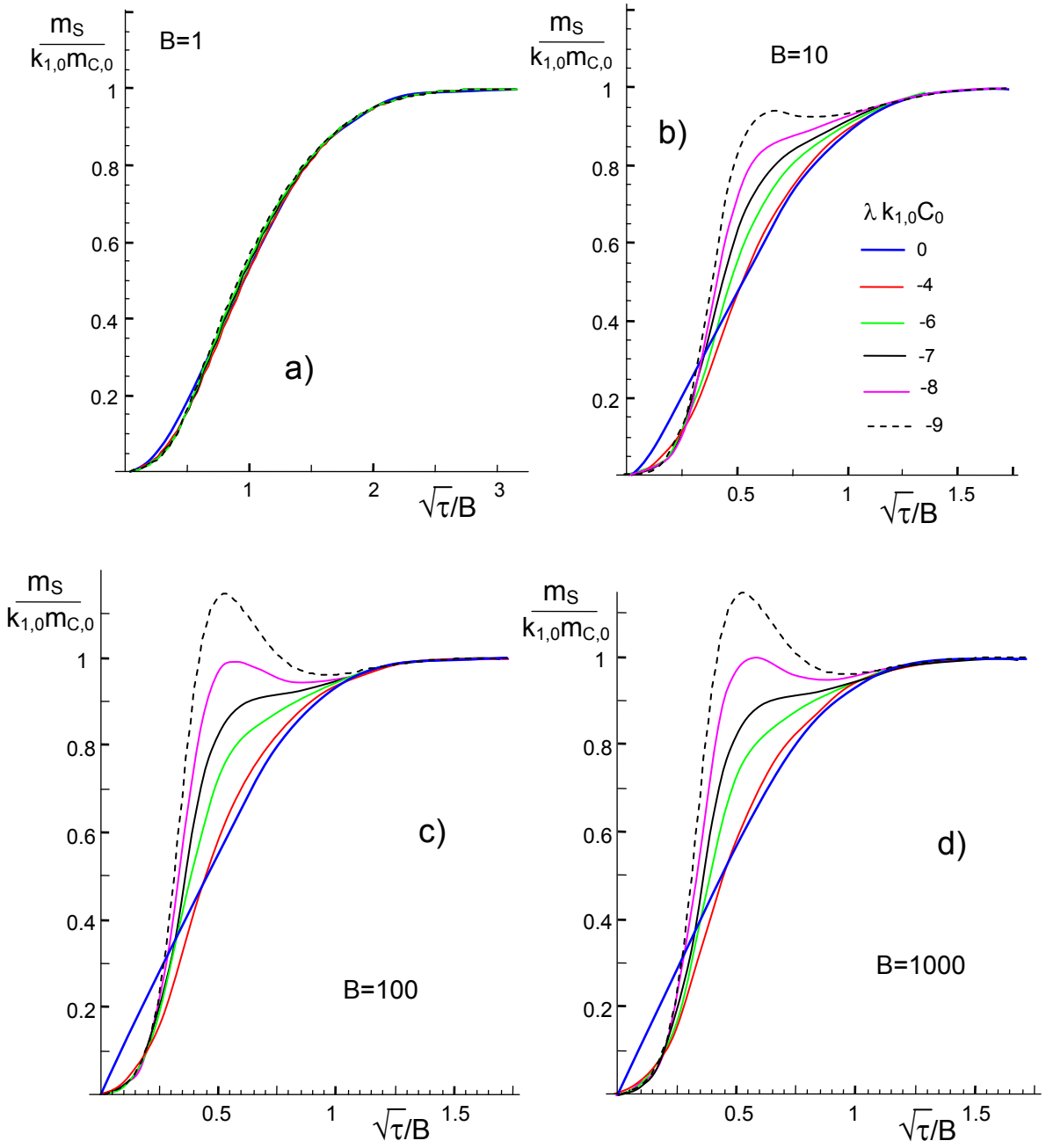

Fig. A1 First-order solution of hydroxyl uptake as a function of stress enhancement, Biot number and time. Note different abscissa scaling in part a).

The effect of swelling stresses on the uptake of hydroxyl water, m_S, via eq.(A7) is shown by first-order computation in Fig. A1. In Fig. A1, the hydroxyl water uptake is plotted as a function of time τ for different values of the parameter λ and several Biot numbers. For strong swelling (large value of parameter $|\lambda k_{1,0} C_0|$) an overshooting of $m_S/(k_{1,0}\, m_C)$ is possible, especially in the case of large Biot numbers.
Finally, Fig. A2 shows details of Fig. A1c for short times and several additional parameters $\lambda k_{1,0} C_0$. From this plot we can see that the change of a nearly linear dependency for $\lambda k_{1,0} C_0$=0 to the curved initial behaviour for compressive values <0 goes continuous with this parameter.

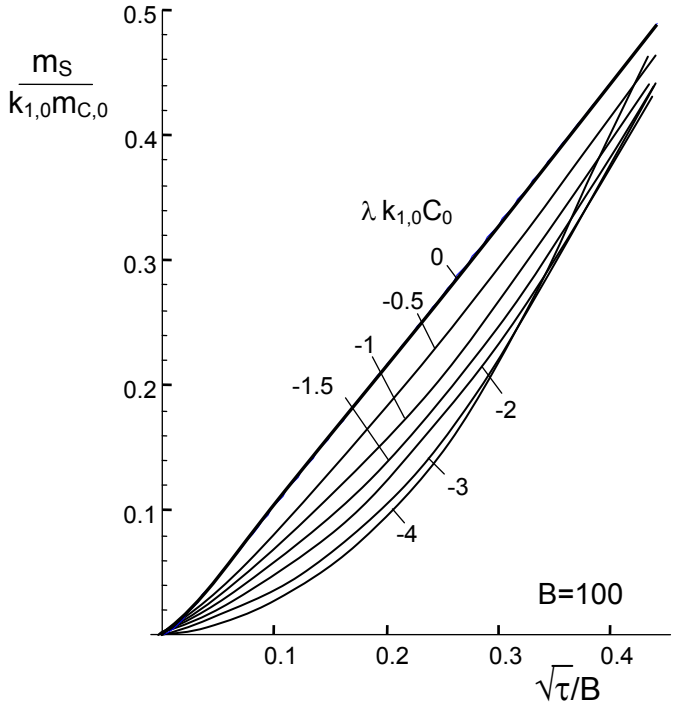

Fig. A2 Short-time details for Fig. A1c.

In context with the results in Fig. A1 it has to be emphasized that the first-order analysis applied for the computations can only identify tendencies of influencing properties (here swelling) but is not appropriated for *quantitative* conclusions or for reliable predictions. A more correct analysis needs numerical evaluations including interactions of stress-enhanced diffusion and stress-enhanced swelling, simultaneously. This has not yet been done.

References

1 Doremus, R.H., Diffusion of water in silica glass, J. Mater. Res., **10**(1995), 2379-2389.

2 S. M. Wiederhorn, G. Rizzi, S. Wagner, M. J. Hoffmann, T. Fett, Diffusion of water in silica glass in the absence of stresses, accepted for J. Am. Ceram. Soc

3 T. Fett, S.M. Wiederhorn, Silica in humid air environment, (I): Diffusion in the absence of stresses, Scientific Working Papers **11**, 2013, KIT Scientific Publishing, Karlsruhe.

4 Carslaw, H.S., Jaeger, J.C. Conduction of heat in solids, 2nd ed. 1959, Oxford Press, London).

5 Munz, D., Fett, T. (1999), CERAMICS, Failure, Material Selection, Design, Springer-Verlag, Heidelberg.

6 R.H. Doremus, Diffusion of Reactive Molecules in Solids and Melts, Wiley, 2002, NewYork.

7 Shelby, J.E., "Density of vitreous silica," J. Non-Cryst. **349** (2004), 331-336.

8 S. M. Wiederhorn, M. J. Hoffmann, T. Fett, Swelling strains from density measurements, Scientific Working Papers **38**, 2015, KIT Scientific Publishing, Karlsruhe.

9 S. M. Wiederhorn, F. Yi, D. LaVan, T. Fett, M.J. Hoffmann, Volume expansion caused by water penetration into silica glass, J. Am. Ceram. Soc. **98** (2015), 78-87.

10 P.G. Shewman, Diffusion in Solids, McGraw-Hill, New York, 1963.

11 Davis, K.M., Tomozawa, M., Water diffusion into silica glass: structural changes in silica glass and their effect on water solubility and diffusivity, J. Non-Cryst. Sol. **185** (1995), 203-220.

12 S. M. Wiederhorn, G. Rizzi, G. Schell, S. Wagner, M. J. Hoffmann, T. Fett, Diffusion of water in silica: Influence of moderate stresses, submitted to J. Am. Ceram. Soc.

13 *Mathematica*, Wolfram Research, Champaign, USA.

14 H. Le Chatelier, *C.R. Acad. Sci. Paris* **99**(1884), 786.

KIT Scientific Working Papers
ISSN 2194-1629

www.kit.edu